

## Article

# Effect of Wettability on Vacuum-Driven Bubble Nucleation

Sushobhan Pradhan <sup>1</sup>, Sage Counts <sup>2</sup>, Charissa Enget <sup>3</sup> and Prem Kumar Bikkina <sup>1,\*</sup>

<sup>1</sup> School of Chemical Engineering, Oklahoma State University, Stillwater, OK 74078, USA; sushobhan.pradhan@okstate.edu

<sup>2</sup> Biosystems and Agricultural Engineering, Oklahoma State University, Stillwater, OK 74078, USA; sacount@ostatemail.okstate.edu

<sup>3</sup> Mechanical and Aerospace Engineering, Oklahoma State University, Stillwater, OK 74078, USA; charissaenget@gmail.com

\* Correspondence: prem.bikkina@okstate.edu; Tel.: +1-405-744-9112; Fax: +1-405-744-6338

**Abstract:** Nucleation is the formation of a new phase that has the ability to irreversibly and spontaneously grow into a large-sized nucleus within the body of a metastable parent phase. In this experimental work, the effect of wettability on the incipitation of vacuum-driven bubble nucleation, boiling, and the consequent rate of evaporative cooling are studied. One hydrophilic (untreated), and three hydrophobic (chlorinated polydimethylsiloxane, chlorinated fluoroalkylmethylsiloxane and (heptadecafluoro-1,1,2,2-tetrahydrodecyl)triethoxysilane) glass vials of different wettabilities were filled with degassed deionized water and exposed to a controlled vacuum inside a transparent desiccator. The vacuum was increased by 34 mbar abs. (1 inHg rel.) steps with 15-min waiting period to observe bubble nucleation. The average onset pressures for gas/vapor bubble nucleation in CM, CF, and HT vials were  $911 \pm 30$ ,  $911 \pm 34$ , and  $925 \pm 17$  mbar abs., respectively. Bubble nucleation was not observed in hydrophilic vial even at 65 mbar abs. pressure. During the vacuum boiling at 65 mbar abs., the average temperatures of water in hydrophilic, CM, CF, and HT vials reduced from room temperature ( $\sim 22.5^\circ\text{C}$ ) to  $15.2 \pm 0.9$ ,  $13.1 \pm 0.9$ ,  $12.9 \pm 0.5$ , and  $11.2 \pm 0.3^\circ\text{C}$ , respectively. The results of this study show that the wettability of the container surface has a strong influence on the onset vacuum for vapor/gas bubble nucleation, rate of vacuum boiling, and evaporative cooling. These findings are expected to be useful to develop wettability-based vacuum boiling technologies.



**Citation:** Pradhan, S.; Counts, S.; Enget, C.; Bikkina, P.K. Effect of Wettability on Vacuum-Driven Bubble Nucleation. *Processes* **2022**, *10*, 1073. <https://doi.org/10.3390/pr10061073>

Academic Editor: Blaž Likozar

Received: 22 April 2022

Accepted: 25 May 2022

Published: 27 May 2022

**Publisher's Note:** MDPI stays neutral with regard to jurisdictional claims in published maps and institutional affiliations.



**Copyright:** © 2022 by the authors. Licensee MDPI, Basel, Switzerland. This article is an open access article distributed under the terms and conditions of the Creative Commons Attribution (CC BY) license (<https://creativecommons.org/licenses/by/4.0/>).

## 1. Introduction

Nucleation is the formation of a new phase that has the ability to irreversibly and spontaneously grow into a larger nucleus within the body of a metastable parent phase. The free energy of the new phase is lower than its parent phase [1]. Vapor bubbles are formed when a pure homogeneous liquid undergoes a phase change or density fluctuations in the liquid. When the bubbles are formed completely within a volatile liquid, it is called homogeneous nucleation. In heterogeneous nucleation, bubbles form at the interface of the parent liquid and the solid phase it is in contact with. If the parent liquid completely wets (contact angle ( $\theta$ ) =  $0^\circ$ ) the solid surface it is in contact with, in the presence of vapor/gas phase, homogeneous bubble nucleation occurs, whereas if the liquid partially wets ( $0^\circ < \theta < 180^\circ$ ) or completely non-wetting ( $\theta = 180^\circ$ ) to the solid surface, heterogeneous nucleation occurs [2]. The most widely used theory to categorize bubble nucleation is the classical nucleation theory (CNT), which describes four different types of nucleation, viz. classical homogeneous nucleation (also referred to as Type I nucleation), classical heterogeneous nucleation (Type II), pseudo-classical nucleation (Type III), and non-classical nucleation (Type IV). In Type I nucleation, bubbles form in the bulk of the liquid and once produced, they rise to the surface of the liquid [3]. In this type of nucleation, it is unlikely to have repeated nucleation sites and a high energy barrier or supersaturation is

required to form a bubble [4]. In Type II nucleation, bubbles form at surface imperfections like pits and cavities present on the surface of the container but without preexisting gas cavities. Type II nucleation occurs at a similar supersaturation level compared to Type I nucleation [5]. In Type III nucleation, bubble nucleation occurs from preexisting gas cavities and is achievable at a significantly lower supersaturation level compared to the Type I and Type II nucleations. The Type IV nucleation also occurs at preexisting gas cavities similar to the Type III nucleation; however, it does not require overcoming any nucleation energy barrier as the radius of curvature of the preexisting gas in the cavities is larger than the critical radius of curvature [3]. A schematic representation of the four types of bubble nucleation is shown in Figure 1.

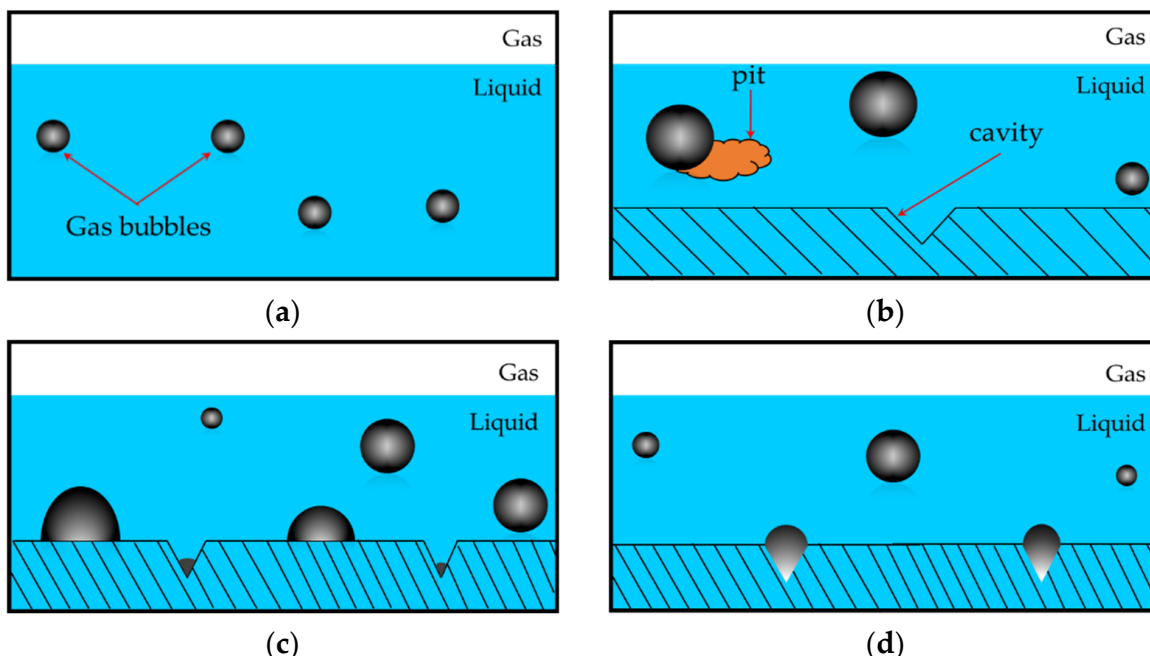


**Figure 1.** A schematic representation of Type I, Type II, Type III, and Type IV bubble nucleation. (a) Type I: Classical homogeneous nucleation; (b) Type II: Classical heterogeneous nucleation; (c) Type III: Pseudo-classical nucleation; and (d) Type IV: Non-classical nucleation.

Wettability, which is the relative preference of a liquid to be in contact with a chemically inert solid surrounded by another fluid, is known to have a strong influence on pressure- and temperature-driven bubble nucleation [6,7]. Eddington and Kenning (1979) studied the effect of contact angles on bubble nucleation and found that enhanced wetting results in a decrease in the total number of bubble nucleation sites through a reduction in effective radii of gas cavities [8]. Tong et al. (1989) showed that for highly wetting liquids, the critical radius of a nucleated bubble is smaller than the cavity radius, and bubbles at critical radii always occur inside the cavities, regardless of the dynamic contact angle values [9]. Nam et al. (2009) reported that the departing bubble diameter was almost three times larger, and the growth period was sixty times longer on the hydrophobic surface than on the hydrophilic surface. The bubble departs from a hydrophobic surface after a short necking period and leaves behind a tiny residual bubble nucleus, on the surface, which further grows in the following cycle without any waiting time. They also reported that smooth hydrophobic surfaces can serve as effective bubble nucleation sites at 6–9 °C of superheat [10]. Sukama et al. (2014) showed that bubble size becomes smaller from hydrophobic to hydrophilic surfaces [11].

The behavior of liquids under sub-atmospheric pressure (negative pressure or vacuum) is of potential research interest as there are important applications such as vacuum boiling, concentrating juices, preservation of proteins, high-rate anaerobic digestion, etc. [12–14]. Kim et al. (2007) studied the growth pattern of vapor bubbles nucleated during pool

boiling at negative pressures. They observed that the radius of bubbles increases with the reduction in system pressure regardless of the type of fluid [15]. Wu and Pan (2002) carried out a molecular simulation study to understand the microscopic processes involved during bubble nucleation in a homogeneous liquid under heating at a constant negative pressure. The simulation results predicted an order of magnitude smaller bubble growth rate compared to the growth rate predicted by the Rayleigh equation. The simulated nucleation rate is three to four orders of magnitude higher than the rate predicted by CNT. They also reported that the nucleation rate decreases with an increase in the magnitude of negative pressure [16].

Very recently, Serdyukov et al. (2022) studied the influence of biphilic surface on heat transfer rate during pool boiling of water in the pressure range of 10–102 kPa. They found that the biphilic surface increases the heat transfer rate up to 3.7 times during the pool boiling process at sub-atmospheric pressures compared to bare surfaces. In addition, at lower pressures (less than 40 kPa), the bubble departure diameter on the biphilic surface is more than 6-times lower compared to the bare hydrophilic surface [17]. Može et al. (2021) studied pool boiling enhancement performances of hybrid-functionalized copper and aluminum surfaces at atmospheric pressure. The hydrophobized copper surfaces covered by microcavities (diameters varied from 40 nm to 2  $\mu\text{m}$ ) enhanced the heat transfer coefficient (HTC) up to 120% and the critical heat flux (CHF) up to 64%, compared to the untreated reference surface [18]. Another study conducted by Može et al. (2021) reported that an etched hydrophobized aluminum surface increased the HTC by 488%, compared to the untreated reference surface. The hybrid-functionalized surface was also observed to cause an earlier transition into a nucleate boiling regime and promote bubble nucleation [19]. It is a well-known fact that hydrophobic surfaces promote bubble nucleation, whereas hydrophilic surfaces increase the CHF during boiling. Liao and Duan (2021) conducted molecular dynamics (MD) simulations to study explosive boiling phenomena on a hybrid hydrophobic–hydrophilic nanostructured surface. The findings of the MD simulation study revealed that the hydrophobic coating could stimulate the formation of bubbles and cause a faster liquid film break-up, resulting in a decrease in the onset temperature of explosive boiling [20]. A study conducted by Regis et al. (2021) to investigate the effect of hydrophilic and hydrophobic surfaces on vacuum-induced surface freezing (VISF) showed that the hydrophobic surface promotes boiling and blow-up phenomena that could result in the formation of unacceptable defects on the glass surface. Although, the hydrophilic surfaces caused an increased risk of fogging on the inner vial surface [21].

Many studies have been conducted on the influence of wettability on bubble nucleation, growth, and detachment processes at pressures above the atmospheric pressure [5–7,22–30]. We recently reported a strong dependency of incipitation pressure of  $\text{CO}_2$  bubble nucleation in water (a two-component system) on the degree of hydrophobicity of the container surface [6]. A limited number of studies have been conducted to investigate the effect of wettability on vacuum boiling at sub-atmospheric pressures despite its various potential practical applications. The objectives of the study are to (a) investigate the effect of wettability on onset pressure for bubble nucleation, and vacuum boiling, and (b) study the change in liquid temperature due to evaporative cooling during vacuum boiling in the hydrophilic and hydrophobic vials. In this work, we report the experimental findings on the effect of wettability on vacuum boiling of water (a single-component system). The rate of evaporative cooling was studied by measuring the change in the liquid temperature during bubble nucleation and vacuum boiling on the surfaces of various wettabilities.

## 2. Materials and Methods

### 2.1. Chemicals and Equipment Details

For the preparation of three different degrees of hydrophobic glass slides and vials used in this study, chlorinated polydimethylsiloxane (CM), chlorinated fluoroalkylmethysiloxane (CF), and (heptadecafluoro-1,1,2,2-tetrahydrodecyl)triethoxysilane (HT) obtained from Gelest Inc. were used. The untreated borosilicate glass slides (make: Fisherfinest)

and vials (make: VWR; capacity: 3.7 mL) were inherently hydrophilic. A vacuum control system that consists of a transparent vacuum desiccator (make: CLEATECH; model: 1300-2-A), a vacuum control unit (make: CLEATECH; model: VCU 120 V), and a deep vacuum pump (make: VIOT; model: VDP5) was used for conducting bubble nucleation experiments under sub-atmospheric conditions. The vacuum desiccator (internal dimensions of 12" W × 12" D × 12" H) is made of 1" thick clear acrylic material with a front-hinged swing door (Type-II) for easier access to samples in the shelves and can withstand 29.8" vacuum in Hg. The vacuum control unit measures the vacuum in inHg and the vacuum units are reported in mbar absolute (abs.) in the following paragraphs. A digital microscope (make: Dino-Lite; model: AM7815MZTL) was used for recording the bubble nucleation process. The change in water temperature during the bubble nucleation and vacuum boiling processes was measured by a dual input RTD thermometer (make: Omega Engineering; model: HH804U), which was connected to a thermal sensor probe (make: Omega Engineering; model: Flexible Hermetic Sealed PFA RTD). The formation of bubbles on the portion of the RTD probe that is immersed in water may result in a decrease in water temperature, particularly in the case of a hydrophilic vial. Therefore, to verify whether there exists any significant influence of the RTD probe on the change in water temperature, a few separate experiments were conducted using a self-adhesive RTD surface sensor (make: Omega Engineering; model: SA1-RTD) attached to the outer wall of the untreated vial. The sensor was connected to a wireless thermocouple (make: Omega Engineering; model: SS-002-0-NA) to record the temperature measurements with the help of an Ethernet gateway (make: Omega Engineering; model: GW-001-2-NA) and an Omega Engineering cloud service. A custom-made goniometer and an atomic force microscopy (AFM) (make: Digital Instruments Multimode AFM; model: MMAFM-2; module: Veeco Nanoscope V) were used for contact angle and the corresponding roughness measurements of the surfaces used in this study.

## 2.2. Chemicals and Equipment Details

The procedures to prepare hydrophilic (untreated glass surface), and various degrees of hydrophobic glass surfaces using siloxanes (CM and CF) and silane (HT) were adopted from our previous study [6]. The experimental procedures are briefly discussed below.

The glass substrates (slides and vials) were rinsed with toluene for siloxane treatments, and with isopropanol for silane treatment. For the siloxane treatments, 10 wt% CM and 10 wt% CF were dissolved in toluene. For silane (HT) treatment, a 95/5 wt% isopropanol/water mixture was prepared and a 0.02 wt% glacial acetic acid was added as a catalyst to the mixture to facilitate the hydrolysis of silane. The solution was kept for 30 min to ensure complete hydrolysis, prior to inserting the glass substrates. Then, the glass substrates were added to the respective solutions and the solutions were thoroughly shaken using a shaking water bath (make: Benchmark Scientific; model: SB-12L) for 60 min at 150 rpm. To remove any unreacted siloxanes, the substrates were rinsed in n-hexane and ethanol. Similarly, the unreacted silanes were removed from the glass substrates by rinsing with ethanol. The untreated glass substrates were inherently hydrophilic. The substrates were rinsed with n-hexane and ethanol to remove any undesired polar and non-polar compounds adsorbed on these surfaces. The treated and untreated substrates were dried in an oven at 105 °C for 30 min.

## 2.3. Static Contact Angle and Roughness Measurements

The wettabilities of the untreated hydrophilic surface and three types of hydrophobic surfaces were characterized using contact angle measurements. The procedure used for static air-water contact angle measurements was reported in our previous study [6]. AFM measurements were conducted to determine the surface roughness of hydrophilic, CM, CF, and HT glass slides and vials.

#### 2.4. Bubble Nucleation Experiments in Vacuum Desiccator

Bubble nucleation experiments were performed in the untreated, CF, CM, and HT glass vials with a working fluid volume of 3 mL. A schematic of the vacuum boiling experimental facility is shown in Figure 2. First, a glass vial of a known wettability was filled with 3 mL of 18.2 MΩ·cm degassed deionized water and placed inside the vacuum desiccator. The deionized water was degassed using the thermal degasification method, i.e., by boiling the deionized water to remove any dissolved gas(es) followed by cooling it down to room temperature in a closed container [31–33]. Then the desiccator was closed, and the vacuum was set at 979 mbar abs. pressure (1 inHg rel.) for 15 min. Then the vacuum was increased by ~34 mbar abs. (1 inHg rel.) steps after every 15 min while observing for any bubble nucleation in the liquid. The process was continued until the first bubble was observed inside the glass vial. After observing the first bubble(s), the vacuum was increased by 102 mbar abs. (3 inHg rel.) to observe bubble growth. The process was continued until vigorous bubble nucleation or boiling was observed. This was until 167 mbar abs. pressure (25 inHg rel.) for all of the experiments. Vigorous bubble nucleation was observed from 133 to 65 mbar abs. pressure (26 to 28 inHg rel.) in the hydrophobic vials. Images of the vials were taken at each vacuum level using the digital microscope. At 65 mbar abs. pressure (28 inHg rel.), videos were recorded to observe the vacuum boiling in the vials. Separate experiments were performed for each of the four types of vials to record the change in temperature, using the RTD input thermometer at every vacuum level during the pressure reduction process.

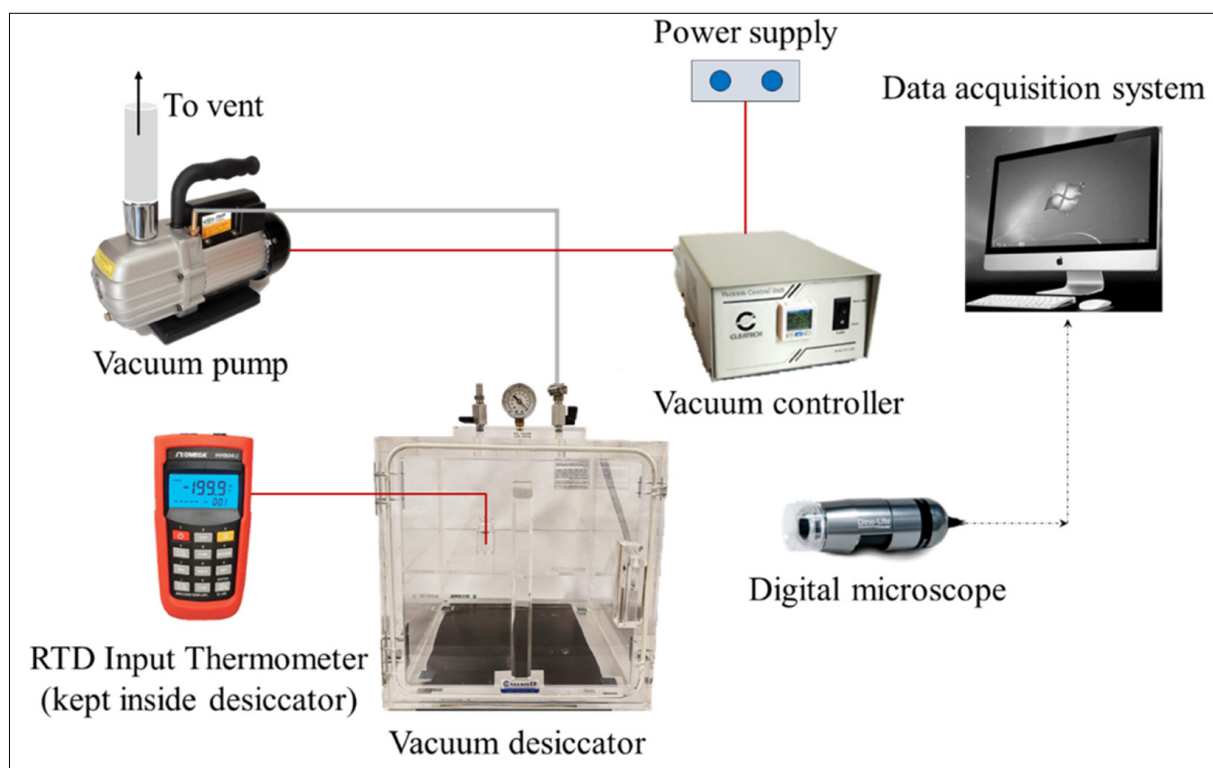


**Figure 2.** Experimental facility used for bubble nucleation experiments at sub-atmospheric pressure.

### 3. Results and Discussion

#### 3.1. Contact Angle and Roughness Measurements

Table 1 presents the average air-water contact angles and surface roughness values with their standard deviations of five and three repeats, respectively, of untreated, CM, CF, and HT treated glass substrates. From Table 1, it can be observed that the contact angle values on CM-, CF-, and HT-treated glass surfaces were increased by 57°, 64°, and 81°, respectively, compared to the untreated surface. As reported in our previous publication [6],

even though there are slight differences in surface roughness, all the surfaces are very smooth (a single-digit nanometer level roughness) and not responsible for the observed bubble nucleation.

**Table 1.** Summary of average contact angles and surface roughness measurements of the hydrophilic and hydrophobic glass substrates.

Surface	Average Contact Angle (°)		Average Roughness (nm)
	Flat Surface	Flat Surface	Vial (Curved) Surface
Untreated	$33.9 \pm 0.4$	$1.1 \pm 0.1$	$3.6 \pm 1.3$
CM	$90.8 \pm 0.8$	$6.6 \pm 0.7$	$6.4 \pm 2.7$
CF	$97.8 \pm 0.4$	$2.9 \pm 0.2$	$4.4 \pm 1.3$
HT	$114.6 \pm 0.75$	$2.4 \pm 0.2$	$7.4 \pm 1$

### 3.2. Vacuum-Driven Bubble Nucleation Results

#### 3.2.1. Effect of Wettability on Onset Vacuum for Bubble Nucleation

Figure 3a–l, shows the bubble nucleation phenomena observed in the four different vials of various degrees of wettabilities. Figure 3a,d,g,j represent the water inside CM, CF, HT, and untreated vials at 1013 mbar abs. pressure (0 inHg rel.) or atmospheric pressure. Figure 3b,e,h, show the first vapor/gas bubble nucleation on the inner surfaces of CF, CM, and HT vials at 911 mbar abs. pressure (3 inHg rel.). As the vacuum increases, newer and larger vapor bubbles were observed to form as can be seen in Figure 3c,f,i for CM, CF, and HT vials, respectively. However, no nucleation was observed on the untreated vial at 911 mbar abs. pressure (Figure 3k). No vapor bubbles formed in the hydrophilic vial even when the vacuum was increased to 65 mbar abs. (28 inHg rel.) (Figure 3l). A video showing the bubble nucleation in CF, CM, and untreated vials (<https://youtu.be/QilmjSg0O5c>, (accessed on 21 December 2020)) and another video showing the bubble nucleation in HT vial ([https://youtu.be/E07DaBB6Q\\_I](https://youtu.be/E07DaBB6Q_I), (accessed on 21 December 2020)) at 65 mbar abs. pressure (28 inHg rel.) can be accessed through the web links provided above or the videos submitted with the manuscript [34,35]. The average onset vacuum (minimum of five experiments) for vapor/gas bubble nucleation on CM, CF, and HT vials were found to be  $911 \pm 30$ ,  $911 \pm 34$ , and  $925 \pm 17$  mbar abs. pressure, respectively.

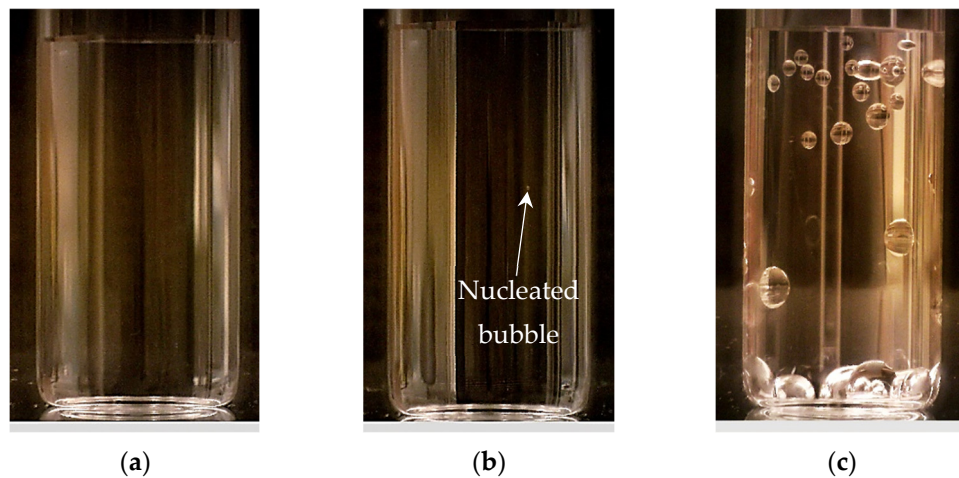


**Figure 3.** *Cont.*

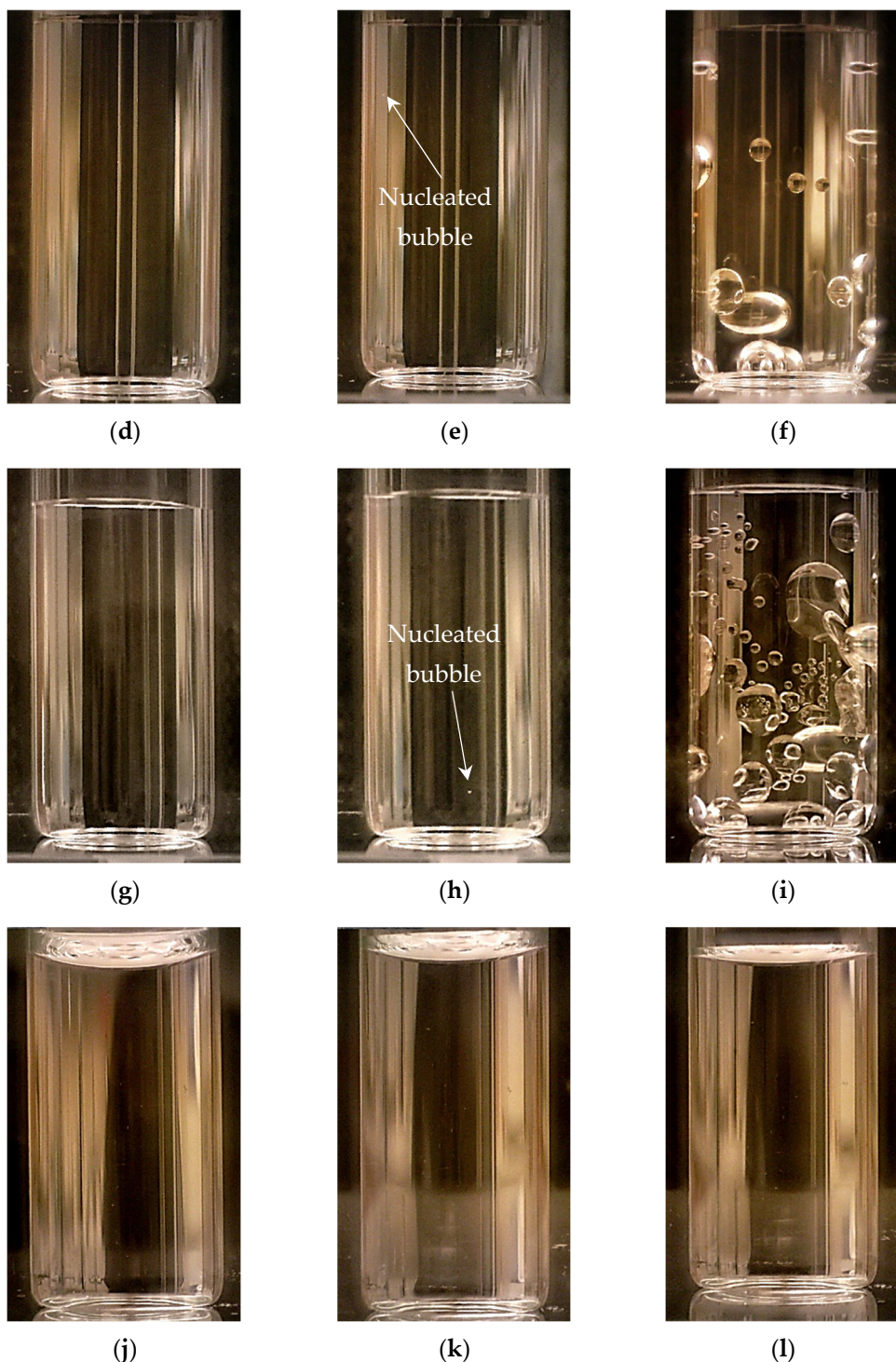


**Figure 3.** Bubble nucleation phenomena in CM, CF, HT, and untreated vials. (a) CM vial at 1013 mbar abs; (b) CM vial at 911 mbar abs; (c) CM vial at 167 mbar abs; (d) CF vial at 1013 mbar abs; (e) CF vial at 911 mbar abs; (f) CF vial at 167 mbar abs; (g) HT vial at 1013 mbar abs; (h) HT vial at 911 mbar abs; (i) HT vial at 167 mbar abs; (j) Untreated vial at 1013 mbar abs; (k) Untreated vial at 911 mbar abs; and (l) Untreated vial at 65 mbar abs.

### 3.2.2. Effect of Wettability on Evaporative Cooling during Bubble Nucleation

The effect of wettability on evaporative cooling during vacuum-driven bubble nucleation was studied by continuously measuring the water temperature using the RTD input thermometer. Figure 4 shows the temperature profiles of water in CM, CF, HT, and

untreated vials from 1013–65 mbar abs. pressure (0–28 inHg rel.). As shown in the figure, the average temperature (of three replicate experiments) vs. vacuum curves can be divided into three stages. In the first stage, i.e., from 1013–302 mbar abs. pressure (0–21 inHg rel.), the decrease in water temperature was very gradual ( $\sim 0.5^\circ\text{C}$ ). In the second stage, i.e., from 268–99 mbar abs. pressure (22–27 inHg rel.), the temperature of water decreased by about  $2^\circ\text{C}$ . However, in the third stage, i.e., at 65 mbar abs. pressure (28 inHg rel.), vigorous vacuum boiling occurred in the three different hydrophobic vials resulting in a sharp decrease in temperature of water. During vacuum boiling, the average temperatures of water in CM, CF, and HT decreased from room temperature ( $\sim 22.5^\circ\text{C}$ ) to  $13.1 \pm 0.9^\circ\text{C}$ ,  $12.9 \pm 0.5^\circ\text{C}$ , and  $11.2 \pm 0.3^\circ\text{C}$ , respectively. However, the corresponding average temperature in the hydrophilic vial only decreased to  $15.2 \pm 0.9^\circ\text{C}$  from the room temperature. It should be noted that bubble nucleation did not occur in hydrophilic vials even at 65 mbar abs. pressure (28 inHg rel.).

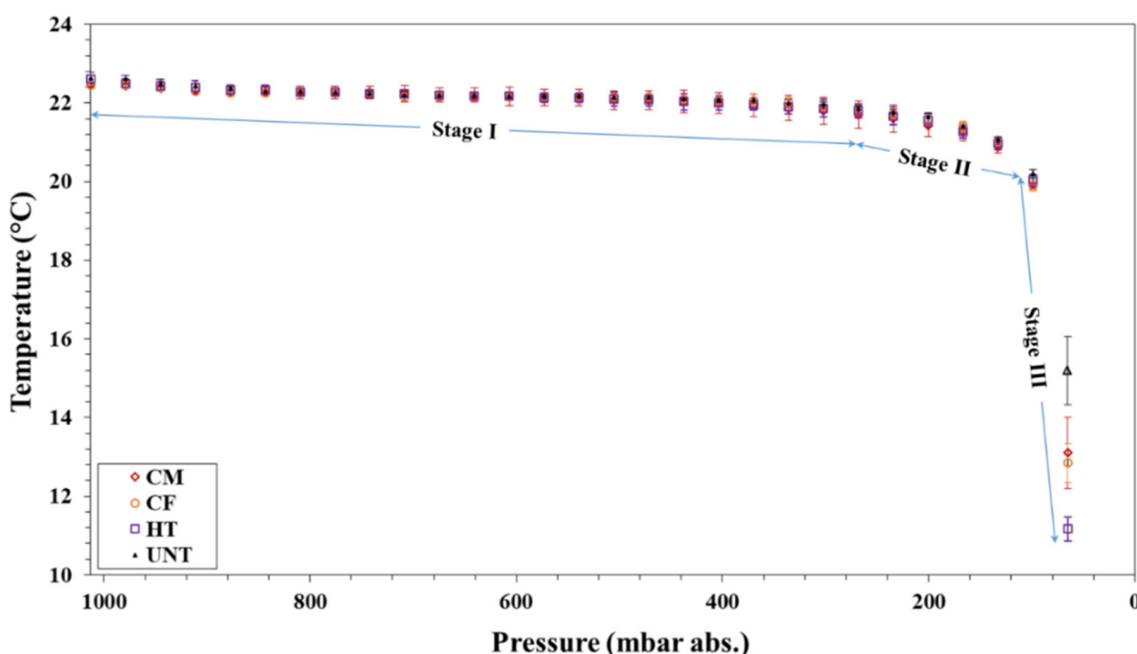


**Figure 4.** Measured temperature vs. vacuum trends of water in hydrophilic (untreated) and hydrophobic (CM, CF and HT) vials.

From the temperature profiles of water in CM, CF, HT, and untreated vials, discussed in the previous section, and the corresponding observed vapor bubble formation rates, it can be inferred that the rate of evaporative cooling is directly related to the rate of vacuum boiling. Since the vapor bubbles were forming in the hydrophobic vials, the process resembles nucleate boiling. However, in the case of water in the hydrophilic vial, no bubble nucleation occurred, hence it is analogous to the case of convective boiling. As it is known, the heat flux is much higher in the case of nucleate boiling compared to convective boiling; higher amounts of water were boiled in the hydrophobic vials compared to the hydrophilic vial. As can be seen in Figure 4, the highest temperature drop was observed in the HT vial followed by CF, CM, and untreated vials. This observation suggests that as the hydrophobicity increases the rate of vacuum boiling, and the associated rate of evaporative cooling increases. It should be mentioned here that accurate temperature measurements of water using an RTD thermometer during vacuum nucleation is a critical challenge, as the formation of bubbles on RTD surfaces may result in a decrease in water temperature, especially in the case of the hydrophilic vial. Therefore, to address this challenge, a self-adhesive RTD surface sensor was installed on the outer wall of the untreated vial to prevent bubble nucleation in water. During the vacuum boiling (65 mbar abs.), the average

temperature in the hydrophilic vial decreased to  $16.2 \pm 0.3$  °C from  $\sim 21.2$  °C, which is close to the temperature observed with the RTD probe present inside the water.

Figure 5 shows the effect of contact angle on the onset pressure for bubble nucleation, and water temperature during vacuum boiling. From Figure 5, it can be observed that the onset nucleation pressure increases with hydrophobicity. In other words, the required level of vacuum for bubble nucleation decreases with hydrophobicity. It should be noted that, as mentioned above, no bubble nucleation was observed in hydrophilic vial even at the highest (i.e., 28 inHg rel.) vacuum applied in this study. In addition, during the vacuum boiling (at 65 mbar abs. pressure (28 inHg rel.)), the average temperatures of water decrease with hydrophobicity due to an increase in the rate of evaporative cooling.

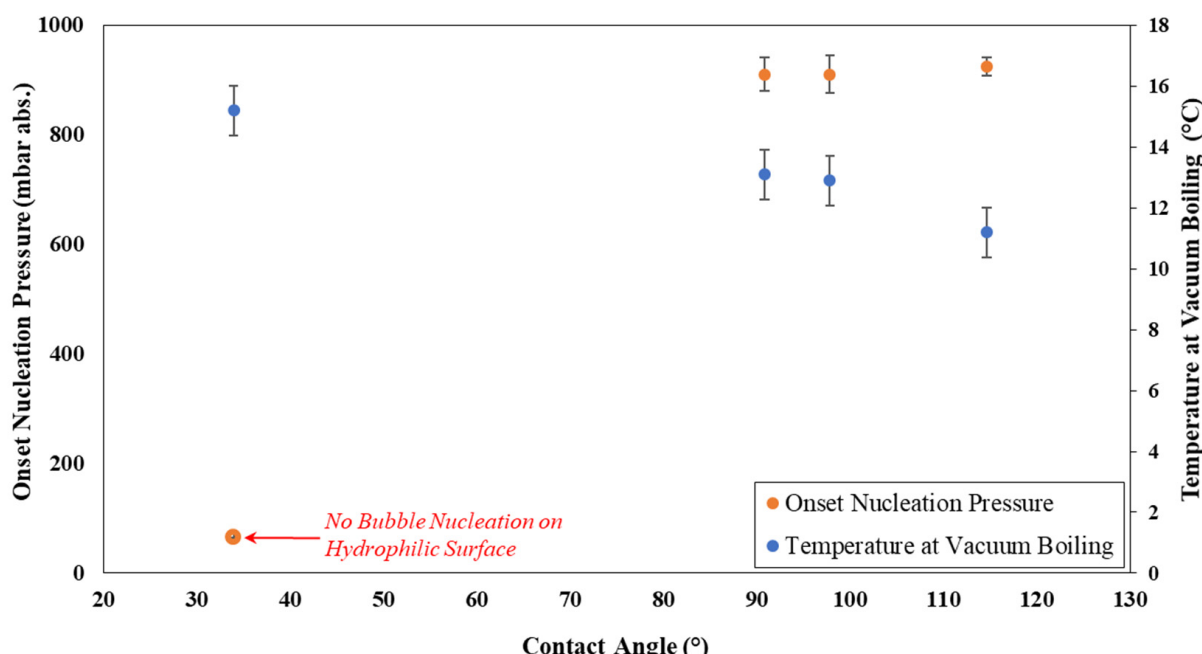


**Figure 5.** Effect of contact angle on the onset pressure for bubble nucleation, and water temperature during vacuum boiling.

#### 4. Conclusions

This present study is carried out to investigate the effect of wettability on vacuum-driven bubble nucleation, and the consequent rate of evaporative cooling. The salient findings of this study are summarized below:

- The wettability of the container surface has a strong influence on the onset vacuum for vapor/gas bubble nucleation, rate of vacuum boiling, and evaporative cooling.
- As the hydrophobicity increases the rate of vacuum boiling, and hence the rate of evaporative cooling increases.
- At higher vacuum levels (stage III in Figure 4), a relatively higher decrease in the temperature of the water was observed in the hydrophobic vials compared to the hydrophilic vials due to an increase in the rate of evaporative cooling.

These findings will be useful for developing wettability-based vacuum boiling technologies.

**Author Contributions:** Conceptualization, P.K.B.; methodology, P.K.B. and S.P.; validation, P.K.B.; formal analysis, S.P. and P.K.B.; investigation, S.P.; resources, P.K.B.; data curation, S.P.; writing—original draft preparation, S.P. and P.K.B.; writing—review and editing, P.K.B. and S.P.; visualization, S.P., S.C. and C.E.; supervision, P.K.B.; project administration, P.K.B.; funding acquisition, P.K.B. All authors have read and agreed to the published version of the manuscript.

**Funding:** The authors gratefully acknowledge Oklahoma State University Startup Funds (AA-1-55622) and American Chemical Society Petroleum Research Fund (PRF# 58560-DNI5) for the financial support for this research project.

**Acknowledgments:** The authors would like to acknowledge Lisa Whitworth (Microscopy Laboratory Manager, Oklahoma State University, Stillwater) for her assistance in conducting AFM measurements, and Elo-oghene Enwa (Graduate Student, School of Chemical Engineering, Oklahoma State University, Stillwater) for his assistance in processing the vacuum boiling videos.

**Conflicts of Interest:** The authors declare no conflict of interest.

## References

1. Okoliecha, C.; Raps, D.; Subramaniam, K.; Altstädt, V. Microcellular to nanocellular polymer foams: Progress (2004–2015) and future directions—A review. *Eur. Polym. J.* **2015**, *73*, 500–519. [[CrossRef](#)]
2. Blander, M.; Katz, J.L. Bubble nucleation in liquids. *AIChE J.* **1975**, *21*, 833–848. [[CrossRef](#)]
3. Jones, S.; Evans, G.; Galvin, K. Bubble nucleation from gas cavities—A review. *Adv. Colloid Interface Sci.* **1999**, *80*, 27–50. [[CrossRef](#)]
4. Diemand, J.; Angélil, R.; Tanaka, K.K.; Tanaka, H. Direct simulations of homogeneous bubble nucleation: Agreement with classical nucleation theory and no local hot spots. *Phys. Rev. E* **2014**, *90*, 052407. [[CrossRef](#)]
5. Vachaparambil, K.J.; Einarsrud, K.E. Explanation of bubble nucleation mechanisms: A gradient theory approach. *J. Electrochem. Soc.* **2018**, *165*, E504. [[CrossRef](#)]
6. Pradhan, S.; Qader, R.J.; Sedai, B.R.; Bikkina, P.K. Influence of Wettability on Pressure-Driven Bubble Nucleation: A Potential Method for Dissolved Gas Separation. *Sep. Purif. Technol.* **2019**, *217*, 31–39. [[CrossRef](#)]
7. Bikkina, P.K.; Pradhan, S. A potential solution for boiling crisis. In Proceedings of the 18th International Topical Meeting on Nuclear Reactor Thermal Hydraulics (NURETH 18), Portland, OR, USA, 18–23 August 2019; American Nuclear Society: La Grange Park, IL, USA, 2019; pp. 1383–1396.
8. Eddington, R.; Kenning, D. The effect of contact angle on bubble nucleation. *Int. J. Heat Mass Transf.* **1979**, *22*, 1231–1236. [[CrossRef](#)]
9. Tong, W.; Bar-Cohen, A.; Simon, T.; You, S. Contact angle effects on boiling incipience of highly-wetting liquids. *Int. J. Heat Mass Transf.* **1990**, *33*, 91–103. [[CrossRef](#)]
10. Nam, Y.; Ju, Y.S. Bubble nucleation on hydrophobic islands provides evidence to anomalously high contact angles of nanobubbles. *Appl. Phys. Lett.* **2008**, *93*, 103115. [[CrossRef](#)]
11. Sakuma, G.; Fukunaka, Y.; Matsushima, H. Nucleation and growth of electrolytic gas bubbles under microgravity. *Int. J. Hydrogen Energy* **2014**, *39*, 7638–7645. [[CrossRef](#)]
12. Han, Y.; Agyeman, F.; Green, H.; Tao, W. Stable, high-rate anaerobic digestion through vacuum stripping of digestate. *Bioresour. Technol.* **2022**, *343*, 126133. [[CrossRef](#)] [[PubMed](#)]
13. Wei, L.; Shirakashi, R. Simulation of air/vacuum desiccation process for high-quality preservation of proteins. *J. Food Process Eng* **2022**, e13962. [[CrossRef](#)]
14. Ermolaev, A.; Krysanov, K.; Tekiev, M.; Silaev, V.; Zaseev, S. Vacuum-evaporative method of juice concentration. In Proceedings of the IOP Conference Series: Earth and Environmental Science, Omsk, Russia, 29–30 March 2021; IOP Publishing: Tokyo, Japan, 2021.
15. Kim, J.; Huh, C.; Kim, M.H. On the growth behavior of bubbles during saturated nucleate pool boiling at sub-atmospheric pressure. *Int. J. Heat Mass Transf.* **2007**, *50*, 3695–3699. [[CrossRef](#)]
16. Wu. A molecular dynamics simulation of bubble nucleation in homogeneous liquid under heating with constant mean negative pressure. *Microscale Thermophys. Eng.* **2003**, *7*, 137–151. [[CrossRef](#)]
17. Serdyukov, V.; Patrin, G.; Malakhov, I.; Surtaev, A. Biphilic surface to improve and stabilize pool boiling in vacuum. *Appl. Therm. Eng.* **2022**, *209*, 118298. [[CrossRef](#)]
18. Može, M.; Vajc, V.; Zupančič, M.; Šulc, R.; Golobič, I. Pool boiling performance of water and self-rewetting fluids on hybrid functionalized aluminum surfaces. *Processes* **2021**, *9*, 1058. [[CrossRef](#)]
19. Može, M.; Vajc, V.; Zupančič, M.; Golobič, I. Hydrophilic and Hydrophobic Nanostructured Copper Surfaces for Efficient Pool Boiling Heat Transfer with Water, Water/Butanol Mixtures and Novec 649. *Nanomaterials* **2021**, *11*, 3216. [[CrossRef](#)]
20. Liao, M.-J.; Duan, L.-Q. Effect of the Hybrid Hydrophobic-Hydrophilic Nanostructured Surface on Explosive Boiling. *Coatings* **2021**, *11*, 212. [[CrossRef](#)]
21. Regis, F.; Arsiccio, A.; Bourlès, E.; Scutellà, B.; Pisano, R. Surface Treatment of Glass Vials for Lyophilization: Implications for Vacuum-Induced Surface Freezing. *Pharmaceutics* **2021**, *13*, 1766. [[CrossRef](#)]
22. Jones, S.; Galvin, K.; Evans, G.; Jameson, G.J. Carbonated water: The physics of the cycle of bubble production. *Chem. Eng. Sci.* **1998**, *53*, 169–173. [[CrossRef](#)]
23. Jones, S.; Evans, G.; Galvin, K. The cycle of bubble production from a gas cavity in a supersaturated solution. *Adv. Colloid Interface Sci.* **1999**, *80*, 51–84. [[CrossRef](#)]
24. Hanafizadeh, P.; Eshraghi, J.; Kosari, E.; Ahmed, W. The effect of gas properties on bubble formation, growth, and detachment. *Part. Sci. Technol.* **2015**, *33*, 645–651. [[CrossRef](#)]

25. Yang, Z.; Dinh, T.-N.; Nourgaliev, R.; Sehgal, B. Numerical investigation of bubble growth and detachment by the lattice-Boltzmann method. *Int. J. Heat Mass Transf.* **2001**, *44*, 195–206. [[CrossRef](#)]
26. Boubendir, L.; Chikh, S.; Tadrist, L. On the surface tension role in bubble growth and detachment in a micro-tube. *Int. J. Multiph. Flow* **2020**, *124*, 103196. [[CrossRef](#)]
27. Georgoulas, A.; Koukouvinis, P.; Gavaises, M.; Marengo, M. Numerical investigation of quasi-static bubble growth and detachment from submerged orifices in isothermal liquid pools: The effect of varying fluid properties and gravity levels. *Int. J. Multiph. Flow* **2015**, *74*, 59–78. [[CrossRef](#)]
28. Pradhan, S.; Bikkina, P.K. An Analytical Method to Estimate Supersaturation in Gas–Liquid Systems as a Function of Pressure-Reduction Step and Waiting Time. *Eng* **2022**, *3*, 116–123. [[CrossRef](#)]
29. Pradhan, S.; Bikkina, P. The Effect of Step-Down Pressure and Wettability on Pressure-Driven Bubble Nucleation for Dissolved Gas Separation. In Proceedings of the 2020 Virtual AIChE Annual Meeting, Virtual, 16–20 November 2020; AIChE: New York, NY, USA, 2020.
30. Pradhan, S. Influence of Wettability on Dissolved Gas Separation, Nucleate Boiling, and Enhanced Oil Recovery. Ph.D. Dissertation, School of Chemical Engineering, Oklahoma State University, Stillwater, OK, USA, 2021.
31. Fuchs, F. Ultrasonic cleaning and washing of surfaces. In *Power Ultrasonics*; Gallego-Juárez, J.A., Graff, K.F., Eds.; Elsevier: Cambridge, UK, 2015; pp. 577–609.
32. Francis, M.J. Effect of degassing on the electrical conductivity of pure water and potassium chloride solutions. *J. Phys. Chem. C* **2008**, *112*, 14563–14569. [[CrossRef](#)]
33. Degassing Water Methods. Available online: <https://www.veoliawatertech.com/en/solutions/technologies/whittier-filtration-separation/degasification> (accessed on 22 April 2022).
34. CF, UNT and CM Vials Containing Degassed and DI Water at 65 mbar Absolute (28 inHg rel.) Pressure. Available online: <https://youtu.be/QilmjSg0O5c> (accessed on 21 December 2020).
35. HT Vial Containing Degassed and DI Water at 65 mbar Absolute (28 inHg rel.) pressure. Available online: [https://youtu.be/E07DaBB6Q\\_I](https://youtu.be/E07DaBB6Q_I) (accessed on 21 December 2020).